The physical properties of glycosyl diacylglycerols. Calorimetric, X-ray diffraction and Fourier transform spectroscopic studies of a homologous series of 1,2-di-O-acyl-3-O-(β-D-ga...

ARTICLE *in* CHEMISTRY AND PHYSICS OF LIPIDS · JULY 2001

Impact Factor: 2.42 · DOI: 10.1016/S0009-3084(01)00153-0 · Source: PubMed

4 AUTHORS, INCLUDING:

David A Mannock
University of Alberta
54 PUBLICATIONS **1,583** CITATIONS
SEE PROFILE

Sol M Gruner
Cornell University
308 PUBLICATIONS **10,622** CITATIONS
SEE PROFILE

ELSEVIER

Chemistry and Physics of Lipids
111 (2001) 139–161

CPL
CHEMISTRY AND PHYSICS OF LIPIDS

www.elsevier.com/locate/chemphyslip

The physical properties of glycosyl diacylglycerols. Calorimetric, X-ray diffraction and Fourier transform spectroscopic studies of a homologous series of 1,2-di-*O*-acyl-3-*O*-(β-D-galactopyranosyl)-*sn*-glycerols☆

D.A. Mannock [a], P.E. Harper [b,1], S.M. Gruner [b,2], R.N. McElhaney [a,*]

[a] *Department of Biochemistry, University of Alberta, Edmonton, Alberta, Canada T6G 2H7*
[b] *Joseph Henry Laboratory, Department of Physics, Princeton University, P.O. Box 708, Princeton, NJ 08544, USA*

Received 26 July 2000; received in revised form 12 April 2001; accepted 12 April 2001

Abstract

We have synthesized a homologous series of saturated 1,2-di-*O*-*n*-acyl-3-*O*-(β-D-galactopyranosyl)-*sn*-glycerols with odd- and even-numbered hydrocarbon chains ranging in length from 10 to 20 carbon atoms, and have investigated their physical properties using differential scanning calorimetry (DSC), X-ray diffraction (XRD) and Fourier-transform infrared (FTIR) spectroscopy. The DSC results show a complex pattern of phase behaviour, which in a typical preheated sample consists of a lower temperature, moderately energetic lamellar gel/lamellar liquid-crystalline (L_β/L_α) phase transition and a higher temperature, weakly energetic lamellar/nonlamellar phase transition. On annealing at a suitable temperature below the L_β/L_α phase transition, the L_β phase converts to a lamellar crystalline (L_{c1}) phase which may undergo a highly energetic L_{c1}/L_α or L_{c1}/inverted hexagonal (H_{II}) phase transition at very high temperatures on subsequent heating or convert to a second L_{c2} phase in certain long chain compounds on storage at or below 4°C. The transition temperatures and phase assignments for these galactolipids are supported by our XRD and FTIR spectroscopic measurements. The phase transition temperatures of all of these events are higher than those of the comparable phase transitions exhibited by the corresponding diacyl α- and β-D-glucosyl glycerols. In contrast, the L_β/L_α and lamellar/nonlamellar phase transition temperatures of the β-D-galactosyl glycerols are lower than those

Abbreviations: α-GlcDAG, α-D-glucopyranosyl diacylglycerol; β-GalDAG, β-D-galactopyranosyl diacylglycerol; β-GlcDAG, β-D-glucopyranosyl diacylglycerol; DSC, differential scanning calorimetry; FTIR, Fourier transform infrared spectroscopy; H_{II}, inverted hexagonal phase; L_α, lamellar liquid-crystalline phase; L_β, lamellar gel phase; L_c, lamellar crystalline phase; L/NL, lamellar/nonlamellar; NMR, nuclear magnetic resonance spectroscopy; PC, phosphatidylcholine; PE, phosphatidylethanolamine; Q_{II}, inverted cubic phase; XRD, X-ray diffraction.

☆ The fatty acyl chains of the lipids used in this study are described by the shorthand notation *N*:0, where *N* denotes the number of carbon atoms per acyl chain with the zero signifying the absence of double bonds.

* Corresponding author. Fax: +1-780-4920095.
E-mail address: rmcelhan@gpu.srv.ualberta.ca (R.N. McElhaney).
[1] Present address: Department of Physics and Astronomy, Calvin College, 3201 Burton SE, Grand Rapids, MI 49546, USA.
[2] Present address: CHESS/Department of Physics, Cornell University, 162 Clark Hall, Ithaca, NY 14853-2501, USA

PII: S0009-3084(01)00153-0

of the corresponding diacyl phosphatidylethanolamines (PEs) and these glycolipids form inverted cubic phases at temperatures between the lamellar and H_{II} phase regions. Our FTIR measurements indicate that in the L_β phase, the hydrocarbon chains form a hexagonally packed structure in which the headgroup and interfacial region are undergoing rapid motion, whereas the L_c phase consists of a more highly ordered, hydrogen-bonded phase, in which the chains are packed in an orthorhombic subcell similar to that reported for the diacyl-β-D-glucosyl-*sn*-glycerols. A comparison of the DSC data presented here with our earlier studies of other diacyl glycolipids shows that the rate of conversion from the L_β to the L_c phase in the β-D-galactosyl glycerols is slightly faster than that seen in the α-D-glucosyl glycerols and much faster than that seen in the corresponding β-D-glucosyl glycerols. The similarities between the FTIR spectra and the first-order spacings for the lamellar phases in both the β-D-glucosyl and galactosyl glycerols suggest that the headgroup orientations may be similar in both β-anomers in all of their lamellar phases. Thus, the differences in their L_β/L_c conversion kinetics and the lamellar/nonlamellar phase properties of these lipids probably arise from subtly different hydration and H-bonding interactions in the headgroup and interfacial regions of these phases. In the latter case, such differences would be expected to alter the ability of the polar headgroup to counterbalance the volume of the hydrocarbon chains. This perspective is discussed in the context of the mechanism for the L_α/H_{II} phase transition which we recently proposed, based on our X-ray diffraction measurements of a series of PEs.

Keywords: Galactolipids; Lipid polymorphism; Lipid thermotropic phase behaviour; Inverted hexagonal phase; Calorimetry; X-ray diffraction; Fourier transform infrared spectroscopy

1. Introduction

There has been considerable interest in the literature in the role of glycolipids in biological membranes. It has long been recognized that many complex glycolipid antigens are involved in the binding of lectins and antibodies at the cell surface (see Varki et al., 1999 for reviews). Our understanding of the participation of carbohydrates at the cell surface in cell adhesion (Vogel et al., 1998; Kulkarni et al., 1999; Handa et al., 2000; Stahn and Zeisig, 2000) and in the recognition events between the host cell membrane and infective agents (Kakimi et al., 2000; Guerrero et al., 2000; Gonzalez-Aseguinolaza et al., 2000; Saubermann et al., 2000; Nishimura et al., 2000) continues to grow, promising new and exciting medical advances. While early studies suggested that only complex glycans were involved in these recognition events, there is new evidence which has shown that some glycolipids, containing only a single sugar headgroup, may play a combination of immunological, regulatory and structural roles in the membrane. The glycosphingolipid, α-D-galactosylceramide, has been shown to be a key activator of triggered cell death (Zhao et al., 1999; Azuma et al., 2000; Osman et al., 2000; Gonzalez-Aseguinolaza et al., 2000; Kitamura et al., 2000; Nicol et al., 2000; Saubermann et al., 2000) and may play a role in the inhibition of virus replication (Kakimi et al., 2000). Several simple glycolipids in a range of biological membranes have also been identified as binding sites for several viruses, including the human immunodeficiency virus (Bhat et al., 1991; Brogi et al., 1995, 1996, 1998; Gadella et al., 1994, 1998) and influenza virus type A (Nakata et al., 2000c). It has been suggested that, in addition to their structural role in the mammalian spermatozoon membranes (Parks and Lynch, 1992), macromolecules capable of binding to the seminolipid (sulfogalactosylalkylacylglycerol) are also responsible for previously undiagnosed infertility in both men (Lingwood et al., 1990) and women (Tsuji et al., 1992). Recent work suggests that this same lipid may be responsible for the binding of the HIV glycoprotein 120 to spermatozoa and subsequent transmission of HIV to the sexual partner (Brogi et al., 1995, 1998). In addition, after ejaculation, the seminolipid is converted by arylsulfatase A present in the seminal fluid, to the β-D-galactosyl-alkylacylglycerol, which has been implicated as a major contributor to membrane fusion during the process of fertilization (Gadella et al., 1994, 1998).

Other glycoglycerolipids, such as the 1,2-di-*O*-acyl-3-*O*-(β-D-galactopyranosyl)-*sn*-glycerols, are found widely in nature as structural components of the photosynthetic membranes of higher plants (Quinn and Williams, 1983), in the cell membranes of prokaryotic blue-green algae and several other microorganisms (Ratledge and Wilkinson, 1988) and in the seeds of cereals, such as wheat and oats (MacMurray and Morrison, 1970; Sahasrabudhe, 1979). These plant galactolipids are the major constituent of a new drug carrier used in pharmaceutical preparations, called Galactosomes® (US patent numbers 5688528; 5716639 and 6022561). It has recently been demonstrated that these galactolipids are also responsible for preventing cell damage and the high resistance to oxidation and heat in the membranes of some microorganisms (Nakata, 2000a,b). Although there have been a number of physical studies of the unsaturated native β-GalDAGs (Sen et al., 1981; Mannock et al., 1985 and references cited therein) and of their hydrogenated derivatives (Sen et al., 1983; Mannock et al., 1985; Lis and Quinn, 1986; Quinn and Lis, 1987), synthetic lipids varying in chain length and structure have not previously been available. In an earlier report (Mannock and McElhaney, 1991), we presented calorimetric and preliminary X-ray diffraction data for a series of even-chain β-GalDAGs, which were prepared as part of a program of synthesis (Mannock et al., 1987, 1990a) and characterization of the physical properties (Mannock et al., 1988, 1990b; Lewis et al., 1990a; Sen et al., 1990) of the family of lipids, termed the glycosyl diacylglycerols. We report here DSC, small-angle XRD and FTIR spectroscopy studies of the thermotropic phase properties of a homologous series of 1,2-di-*O*-acyl-3-*O*-(β-D-galactopyranosyl)-*sn*-glycerols containing both odd and even numbered linear, saturated acyl chains.

2. Materials and methods

The β-GalDAGs used in this study were synthesized according to literature methods (Kaplun et al., 1977; van Boeckel et al., 1985; Mannock et al., 1987) via the 3-*O*-(2,3,4,6-tetra-*O*-acetyl-β-D-galactopyranosyl)-*sn*-glycerol ($[\alpha]_D^{22} = -6.5$, (c1, $CHCl_3$), lit -6.7 (c0.2, $CHCl_3$), Kaplun et al., 1977; -5.9, (c0.17, $CHCl_3$) Bashkatova et al., 1973) or the corresponding syrupy tetrabenzyl diol ($[\alpha]_D^{22} = -5.0$, (c7, $CHCl_3$), as prepared by Gent and Gigg (1975) using odd- and even-chain fatty acids of 10–20 carbons atoms (Nuchek Prep., Elysian, MN). The chemical structure of the lipids prepared here is shown in Fig. 1. The conditions used for the acylation of the above diols were similar to those described earlier (Mannock et al., 1987, 1990a), except that the amount of dicyclohexyl carbodiimide was doubled and the reaction time was extended until thin-layer chromatography (3:1 v/v, ether:hexane) showed that the reaction was complete. The resulting peracetylated lipids were purified on a silica gel column (Davisil, 200–425 mesh, Aldrich-Sigma, St. Louis, MO) eluted with a gradient of carbon tetrachloride/diethyl ether. The β-GalDAG peracetates were crystallized from methanol and gave the following analytical measurements using a Thomas Hoover capillary melting point apparatus and a Perkin–Elmer 241 polarimeter: di-16:0: m.p. 45.5–46.5°C, $[\alpha]_D^{22} = -0.9$ (c1, $CHCl_3$); lit. m.p. 45–46°C, $[\alpha]_D^{22} = -0.61$ (c0.32, $CHCl_3$; Bashkatova et al., 1973); m.p. 45–46°C, $[\alpha]_D^{22} = -0.7$ (c0.1, $CHCl_3$; Kaplun et al., 1978); di-18:0: m.p. 61–62.5°C, $[\alpha]_D^{22} = -1.27$ (c1, $CHCl_3$); lit. m.p. 61.5–62.5°C, $[\alpha]_D^{22} = -1.7$ (c1.5 $CHCl_3$:MeOH, (2:1 (v/v); Batrakov et al., 1976). Some of the shorter chain compounds were synthesized via 3-*O*-(2,3,4,6-tetra-*O*-benzyl-β-D-galactopyranosyl)-*sn*-glycerol (Gent and Gigg, 1975). The acetate or benzyl groups were deprotected in the usual way (Gent and Gigg 1975; Mannock et al., 1987, 1990a) and the deprotected lipids were applied to a column of Davisil (200–

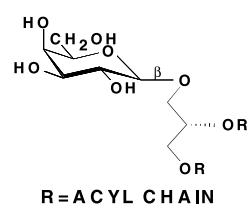

Fig. 1. The chemical structure for the 1,2-di-*O*-acyl-3-*O*-(β-D-galactopyranosyl)-*sn*-glycerols used in this study.

425 mesh) slurried in chloroform and eluted with a gradient of chloroform and acetonitrile in order to remove trace amounts of dicylohexylurea. The purified lipids were eluted from the column at a ratio of 2:1, v/v chloroform:acetonitrile and were crystallized first from acetone, then from methanol or methanol and water, to give the pure unprotected β-GalDAGs which showed melting points (sintering points) and optical rotations as follows: di-20:0, ($\approx$100) 149–50; di-18:0, ($\approx$98) 150–151°C; di-16:0, ($\approx$94) 143–5°C, $[\alpha]_D^{22} = -2.7$; di-14:0, ($\approx$86) 139–41°C, $[\alpha]_D^{22} = -2.1$; di-13:0, $[\alpha]_D^{22} = -3.3$ and di-12:0, ($\approx$75) 135–7°C, $[\alpha]_D^{22} = -4.5$ (all c1, chloroform); lit. di-16:0, m.p. (100) 147–149°C, $[\alpha]_D^{22} = -2.3$ (c1.5, $CHCl_3$:MeOH (2:1, v/v), Batrakov et al., 1976); m.p. 149–150°C, $[\alpha]_D^{22} = -4.0$ (c0.5, $CHCl_3$; Gent and Gigg, 1975); m.p. = 141–142°C, $[\alpha]_D^{22} = -6.53$ (c0.71, $CHCl_3$; Bashkatova et al., 1973); m.p. 142–143°, $[\alpha]_D^{22} = -6.6$ (c0.1, $CHCl_3$; Kaplun et al., 1978); m.p. (91–93) 152–154°C, $[\alpha]_D^{22} = -2.04$ (c4.7, pyridine). Estimations of the purity of the final lipids (as their acetates in $CDCl_3$) using ^{1}H-NMR ranged from 96 to 99% β-GalDAG, the remaining percentage being the α-anomer, which proved more difficult to remove chromatographically in the shorter chain compounds. The lipids were then lyophilized from benzene:methanol (9:1, v/v) for long-term storage prior to the physical studies of their aqueous dispersions. All solvents were reagent grade and were redistilled before use. Additional analytical measurements for the β-GalDAGs can be found below:

^{1}H-NMR: di-16:0 peracetate (200 Mhz, $CDCl_3$): 0.85 ppm, 6H $2CH_3$; 1.25 ppm, 44H $(CH_2)_{C4-C\omega-1}$, 1.6 ppm, 4H CH_2 @ C3, 2.0 ppm, 12H four acetate groups, 2.3 ppm, 4H CH_2 @ C2, 3.5–5.3 ppm 12H from $H_{1\text{-}6A,B}$, $H_{1'A,B}$, $H_{3'A,B}$, $H_{2'}$. H_1 4.54 ppm (7.5 Hz).

^{1}H-NMR: di-15:0 unprotected (500 Mhz, DMSO-d_6): 0.85 ppm, 6H $2CH_3$; 1.23 ppm, 40H $(CH_2)_{C4-C\omega-1}$, 1.5 ppm, 4H CH_2 @ C3, 2.26 ppm, 4H CH_2 @ C2, 3.3–5.2 ppm 12H from $H_{1\text{-}6A,B}$, $H_{1'A,B}$, $H_{3',B}$, $H_{2'}$ H_1 4.52 ppm (7.5 Hz).

Elem. Anal. Unprotected di-16:0-β-GalDAG. $C_{41}H_{78}O_{10}$, Expected C 67.36%, H 10.75%, O 21.88%. Observed C 66.64%, H 10.46%, O 21.88%.

All reactions were monitored using 0.5 mm thick Whatman K6 silica gel G60 5 × 10 cm thin-layer chromatography plates.

DSC measurements were performed with a Perkin–Elmer DSC-2C calorimeter equipped with a thermal analysis data station using Perkin–Elmer TADS software. Lipid samples for DSC were prepared and quantified as reported earlier (Mannock et al., 1988, 1990b). The lipid samples were repeatedly heated and cooled to ensure complete hydration and then DSC thermograms were recorded between −3 and 97°C.

Samples for XRD were prepared by transferring 3–5 mg of dry lipid into a thin-walled X-ray glass capillary (1.5 mm). Excess deionized water (one to two times the lipid weight) was added and the two components were mechanically mixed. The capillary was then sealed with 5-min epoxy and the sample was repeatedly heated and cooled between 20 and 90°C to further mix the water and lipid. Small-angle X-ray methods are as described in Lewis et al. (1989). Briefly, X-rays were generated on a rotating anode X-ray generator. The beamline was equipped with single-mirror Franks optics, a thermostated (−30 to 100°C) specimen stage and an area X-ray detector. The area detector was either the area detector described in Reynolds et al. (1978) or the successor detector in which the silicon diode vidicon camera was replaced with a slow-scan CCD camera (the 'intensifier/lens/CCD' camera described in Tate et al. (1997)).

A typical thermal protocol involved incubating the sample in the X-ray sample stage at −10°C for 30 min followed by annealing the sample at 23°C until the stable phase was fully formed. This was followed by heating the sample in 2 or 5°C steps, to a maximum of 95°C. Each step consisted of setting the temperature of the specimen stage, waiting 30–60 min for the sample to equilibrate and then taking a diffraction pattern of 2–3 min in duration. After the maximum temperature had been reached, the sample was then stepped back

down in temperature using an analogous step sequence. Comparisons of the heating and cooling X-ray diffraction profiles show substantial supercooling of the inverted cubic phases in the cooling direction. This hysteresis is visible even at the slowest rates of temperature change used here. For samples which showed the same Q_{II} phase, differences in the unit cell spacings were frequently seen if the equilibration times were too short, indicating that bulk water could not be drawn into the aqueous pore fast enough to permit the maximum swelling of the unit cell to occur. In general, within a given phase, the unit cell spacings are more reliable when the unit cell is shrinking than when it is expanding, since the active extrusion of water out of the unit cell and into a coexisting bulk water phase seems to be faster than the diffusion of water from the bulk into the lipid phase. In view of the above behaviour, it is worth emphasizing that the measurements presented here were not taken under true equilibrium conditions and that the dimensions and the type of phase structure seen under true equilibrium conditions may differ from those presented here.

Samples typically exhibited only a few orders of diffraction. Diffraction patterns with spacings which could all be fit to the sequence 1:2:3 . . . and with unit cells in the range of 40–70 Å indicated the existence of lamellar phases. Spacings in the sequence $1:\sqrt{3}:2:\sqrt{7}\ldots$ and unit cells of 60–80 Å were assumed to be characteristic of inverse hexagonal phases. Cubic phases have orders with spacings that are a subset of the sequence $\sqrt{(h^2+k^2+l^2)}$, where h, k and l are integers. The assignment of the specific cubic phase is frequently difficult and ambiguous (Hajduk et al., 1994) and is limited by the number of observed orders. The specific inverted cubic phase assignments given below were based on a limited number of diffracted orders. When such a phase assignment was made, sufficient reflections were present to tentatively assign a cubic phase lattice to the sample under those conditions, despite the absence of a full set of reflections necessary for a definitive structural analysis. When no identification was given for a particular temperature region of these lipids, it was unclear what phase(s) might or might not be present. What was unequivocal, under these circumstances, was that these phases could be reliably determined *not* to be a single lamellar or inverted hexagonal phase. X-ray spacings are generally accurate to ± 0.5 Å and temperatures of the X-ray specimen stage were controlled to better than ± 0.5°C.

Samples for the infrared spectroscopic measurements were prepared by thoroughly mixing 2–3 mg of the freeze-dried lipid with 10–20 μl of D_2O and squeezing the paste formed between two CaF_2 plates to form a 12-μm thick film. The plates were mounted on the sample holder and the sample heated in situ to temperatures above that of the gel/liquid-crystalline phase transition of the lipid to ensure complete hydration. The samples were then annealed under conditions appropriate for the formation of the lipid phase of interest, as described in the text. Infrared spectra were recorded at a resolution of 2 cm^{-1} on a Digilab FTS-40 spectrometer equipped with a deuterated triglycine sulfide detector using data acquisition and data processing parameters similar to those previously reported (Mantsch et al., 1985; Lewis et al., 1990b).

3. Results

3.1. Thermotropic phase behaviour

In order to provide a basic overview of the effect of scan rate on the thermotropic phase behavior of these β-GalDAGs, all lipid samples were initially measured by DSC using a range of heating and cooling rates (20–0.3°C/min) over the temperature range −3 and 97°C, as was previously reported by us for the α- and β-GlcDAGs (Mannock et al., 1988, 1990a). This data consisted of complex heating and cooling thermograms (Fig. 2), which was used to estimate the rate of the metastable to stable phase conversion processes at each lipid chain length. These experiments were also used in the design of the DSC experiments required to form and study any metastable phases, as required for a complete characterization of the thermotropic phase behaviour of these β-GalDAGs (Fig. 3 and Table 1).

Fig. 2 clearly shows the rapid rate of the metastable to stable phase conversion process in these β-GalDAGs (in Fig. 2 the metastable gel phase is denoted by an asterix, whereas the stable L_c phase is denoted by the symbol ¤). In the case of the shorter, even-chain lipids, the formation of the stable phase is so fast that the conversion occurrs either at very slow cooling rates (typically 0.3°C/min) or immediately upon reheating of the sample from the supercooled metastable phase. It is also evident that the difference in the rate of the conversion process between odd and even-numbered β-GalDAGs is not as great as that observed in our earlier studies of the β-GlcDAGs and α-GlcDAGs (Mannock et al., 1988, 1990b).

In order to properly define the conditions under which the stable and metastable phases of the β-GalDAGs were formed, the lipid samples were cooled either to − 3°C to encourage nucleation of the stable gel phase, or they were cooled to a few degrees below the transition to the metastable phase, but above the nucleation temperature of the stable phase. The nucleation temperature was determined in a few representative hydrocarbon chain lengths by systematically reducing the lower temperature limit to which the sample was cooled and then by immediately reheating the sample at 1°C/min to the upper temperature limit of 97°C. This iterative procedure permitted the nucleation temperature of the lipid sample to be crudely estimated under our conditions by the appearance of an endothermic contribution on reheating the sample, occurring at the same temperature as that of the stable gel phase chain melting phase transition. In order to monitor the conversion process under a standard set of conditions, as was performed in our earlier studies of the corresponding α- and β-GlcDAGs, all β-GalDAG samples were cooled to − 3°C to initiate nucleation of the stable phase, followed by different periods of storage at 22°C. Under these conditions, the minimum time required for the stable gel phase to completely reform in the di-19:0-β-GalDAGs is ≈ 30 days, as determined by estimates of the sample enthalpy from an extensive series of time course experiments. In order to investigate the possible formation of additional stable, subgel-like phases, a duplicate set of galactolipid DSC samples were stored at 22°C for up to 2 years prior to reheating. Additional samples were also subsequently stored at 4°C for up to 60 days after the initial nucleation and storage at 22°C was completed in order to induce the formation of additional stable gel phases. Similar protocols were utilized with each physical technique.

3.2. Metastable mesophase region

Representative thermograms of the series of β-GalDAGs with odd and even chain lengths ranging from 10 to 20 carbon atoms, in which the metastable mesophases and the stable lamellar crystalline phases have been isolated, are shown in Fig. 3. (Unless stated otherwise, the scan rate in Fig. 3 was always 1°C/min.) The corresponding thermodynamic data appears in Table 1. On cooling, the short (di-10:0 to 13:0) chain compounds all show evidence of a weakly energetic exothermic event, the temperature of which is slightly dependent on the cooling rate. This is followed by a second, more energetic, exothermic event at lower temperature. Immediate reheating from a

Fig. 2. DSC thermograms of a series of 1,2-di-*O*-acyl-3-*O*-(β-D-galactopyranosyl)-*sn*-glycerols with acyl chain lengths ranging from 10 to 20 carbon atoms. Each sample was initially heated and cooled at scan rates between 20 and 0.31°C/min over the temperature range − 3 to 97°C (except for di-10:0, which was − 10 to 97°C). In each panel, the top four or five thermograms are heating thermograms, whereas the bottom thermogram is a cooling thermogram obtained at 1°C/min. The presence of a metastable gel phase is indicated by an asterix (*), whereas the presence of a stable L_c phase is marked by the symbol (¤). The sequence of thermograms in each panel is from top to bottom. Note that the unusual behaviour of the di-16:0 sample reflects a gradual increase in the nucleation temperature with increasing chain-length, since samples of the di-16:0 lipid heated and cooled between 17 and 97°C at the same scan rates show almost no conversion to the L_c phase. Thus, the exothermic event which changes temperature with heating rate on reheating these lipid samples following nucleation, must correspond to the L_β/L_c conversion process. Furthermore, at chain-lengths longer than 16 carbon atoms, an increase in the nucleation temperature, combined with the slower kinetics of the L_β/L_c conversion process and the decrease in the temperature range over which the conversion to the L_c phase can occur, leaves a greater proportion of the L_β phase during the heating scan.

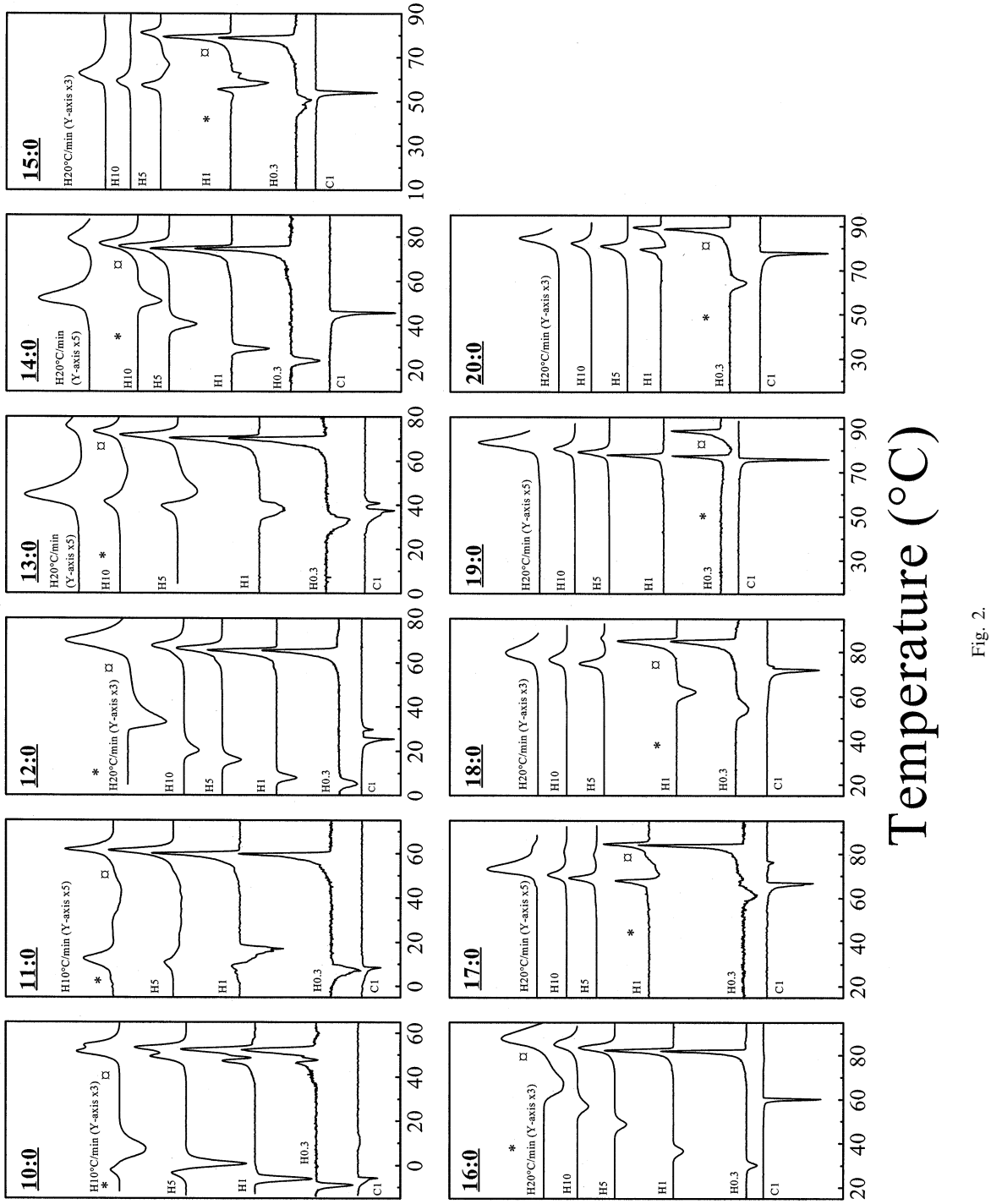
10:0
11:0
12:0
13:0
14:0
15:0
16:0
17:0
18:0
19:0
20:0
H10°C/min (Y-axis x3)
H10°C/min (Y-axis x5)
H20°C/min (Y-axis x3)
H20°C/min (Y-axis x5)
H20°C/min
(Y-axis x5)
H20°C/min (Y-axis x3)
H10
H5
H1
H0.3
C1
Endothermic
Temperature (°C)

Fig. 2.

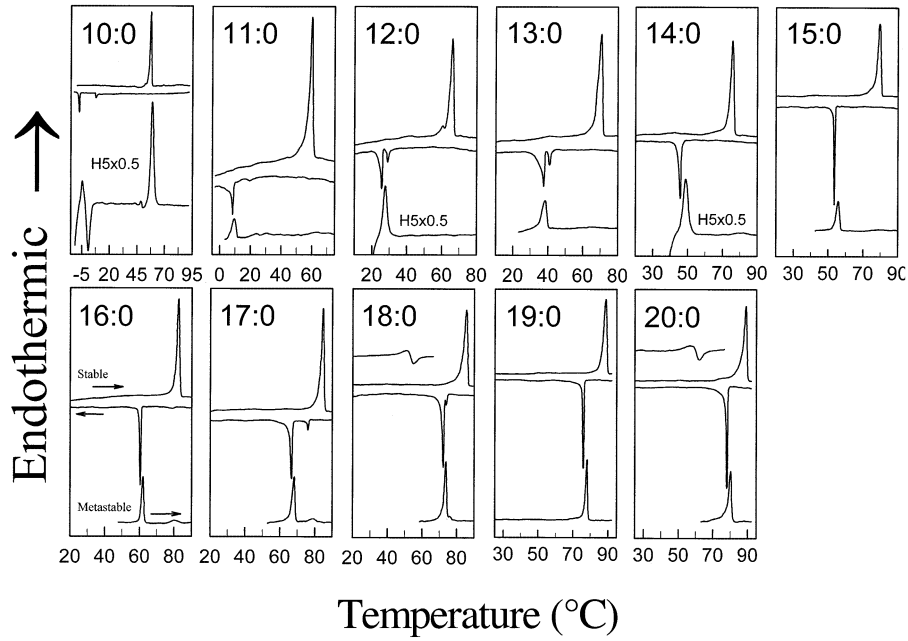

Fig. 3. DSC thermograms of a series of 1,2-di-*O*-acyl-3-*O*-(β-D-galactopyranosyl)-*sn*-glycerols with acyl chain lengths ranging from 10 to 20 carbon atoms showing a comparison of stable and metastable phase behaviour. Two sets of experiments are reported here. Each annealed sample was initially heated and cooled at 1°C/min (top and middle thermogram). Each sample was then reheated to 97°C for a second time. They were then cooled to 5–10°C below the L_α/L_β phase transition and immediately reheated to 97°C for a third time and recooled to the lower temperature limit (-3°C). Where possible, the third reheating scans (lower curve) were obtained at a heating rate of 1°C/min except for 10:0, 12:0 and 14:0, which were heated at 5°C/min. (These curves are reduced along their vertical axes by one half in the above panels). An alternative protocol was also attempted in which the first cooling was stopped just below the L_α/L_β phase transition and immediately reheated to 97°C (second heating scan) followed by cooling to the lower temperature limit. The thermograms obtained by this shortened procedure were superimposable with those obtained by the longer procedure described above. The arrows on each panel indicate the direction of temperature change for each scan. See legend to Fig. 2 for additional comments.

few degrees below the more energetic peak shows that the main phase transition is reversible (except in the case of di-10:0 at scan rates < 1°C/min). However, the minor higher temperature event(s) are only seen on reheating at fast scan rates under these circumstances and those events show no correspondence to the peaks seen on cooling. In the medium chain compounds (di-14:0 to 16:0), the highly energetic, lower temperature transition persists and is reversible, but the weakly energetic, high temperature peak evident at shorter chain lengths disappears except in the case of the di-16:0 compound, where a new broad, weakly energetic, reversible event is visible at higher temperature. Corresponding XRD measurements (Fig. 4 and Table 2) of the short and medium chain β-GalDAGs confirm the pattern of thermal events seen by DSC and show that the phases on either side of the main transition have lamellar characteristics (see Section 2) and that the d-spacing decreases by ≈ 2–3 Å across the transition on heating.

In order to further investigate the structure of the lamellar phases formed by these lipids, Fourier transform infrared (FTIR) spectroscopic measurements were performed in both the heating and cooling modes on three β-GalDAGs (14:0, 15:0, 18:0). These measurements showed transition temperatures that were in agreement with those obtained by DSC and XRD. As the spectra for these lipids were similar, only data for the di-15:0 compound is presented here. Representa-

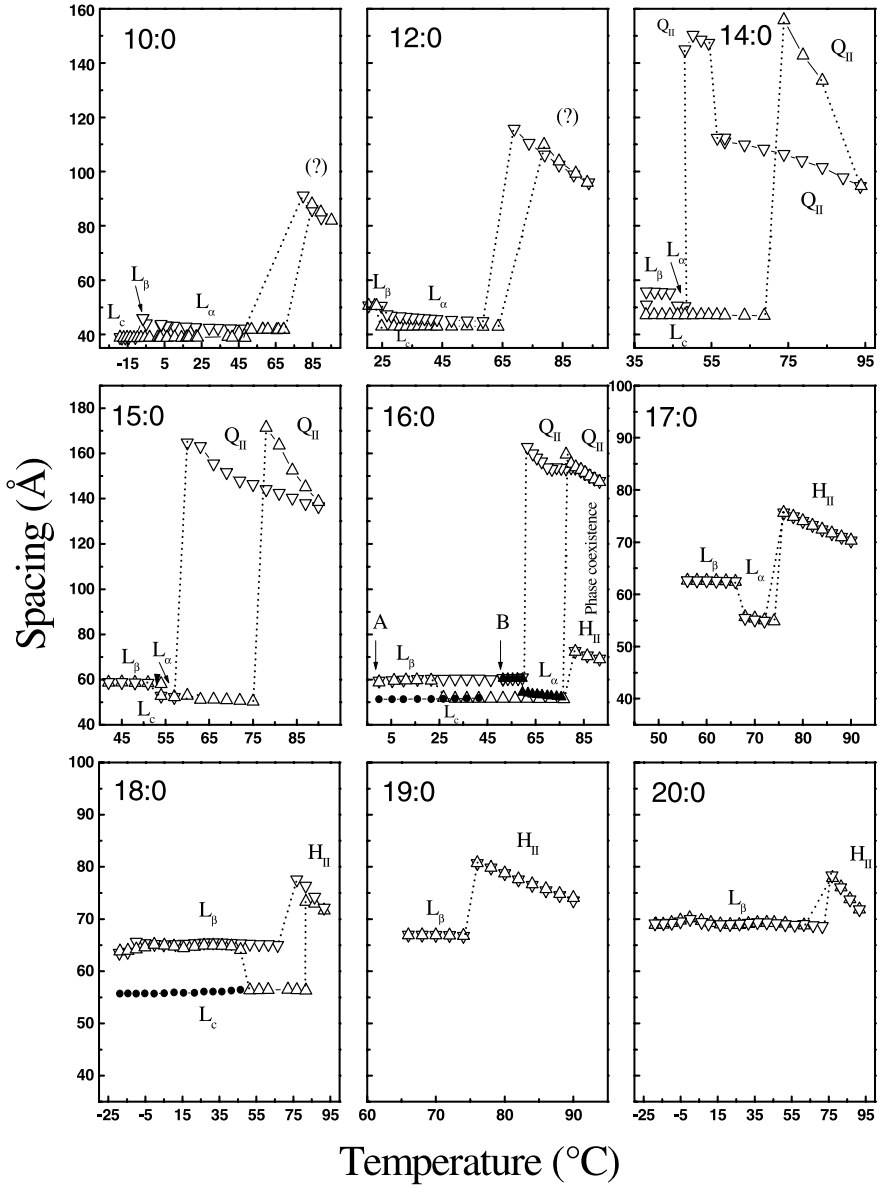

Fig. 4. Plots of the cell lattice parameter (Å) measured as a function of temperature for selected 1,2-di-*O*-acyl-3-*O*-(β-D-galactopyranosyl)-*sn*-glycerols. Up and down arrows (△, ▽) indicate the direction of temperature change. Hollow symbols indicate initial heating and cooling experiments, filled symbols (▲, ●) indicate additional heating experiments which were performed to isolate one or more phases, For example, in the panel for the di-16:0-lipid, the ● represents experiments designed to isolate the L_c phase which were started at (A) 0°C. In contrast the ▲ represents an experiment, started at (B) 50°C, which was used to isolate the L_β phase. Where a filled set of symbols runs into a hollow set of symbols there is a duplicate set of data points from a second experiment underneath the first set, but only one data set is shown for clarity. We have tentatively assigned phase structures using a combination of low-angle XRD and FTIR measurements and have provided labels for these tentative assignments for each lipid chain length.

Table 1
Thermodynamic properties of the various phase transitions of the β-D-galactosyl diacylglycerols[a]

Acyl chain length	L_{c2}/L_{c1}		L_{c1}/L_{α}		L_{β}/L_{α}		L_{α}/NL	
	T_m	ΔH	T_m	ΔH	T_m	ΔH	T_m	ΔH
(A) The phase transitions seen on heating								
10	–	–	57.5	19.8	−6.9	–	[a]	–
11	–	–	60.0	19.0	9.5	2.7	[a]	–
12	–	–	65.3	18.2	26.8	4.7	[a]	–
13	–	–	70.3	18.1	38.5	5.9	[a]	–
14	–	–	75.4	20.7	48.7	6.8	80.6[b]	0.4
15	–	–	79.3	21.7	55.5	8.1	≈75[b,c]	–
16	–	–	82.3[d]	23.0	61.6	8.7	80.7[b,c]	1.3
17	–	–	84.3[d]	22.6	67.9	10.3	78.1[c]	1.1
18	45–62[f]	–	85.0[d]	25.7	73.5	11.1	76.0[e]	1.0
centre@53								
19	–	–	88.7[d]	26.1	77.8[e]	13.2	77.8[e]	13.2
20	50–70[f]	–	89.0[d]	26.8	80.0[e]	14.3	80.0[e]	14.3
centre@61								

(B) The phase transitions seen on cooling

Acyl chain length	L_{α}/L_{β}		NL/L_{α}	
	T_m	ΔH	T_m	ΔH
10	−7.7	−2.8	7.7[g]	–
11	8.1	−3.1	19.5[g]	–
12	25.2	−4.9	28.6[g]	−1.0
13	37.3	−6.3	40.6[g]	−0.8
14	45.5	−8.5	46.6[g]	–
15	53.6	−9.5	–	–
16	60.1	−9.6	78.4[g,h]	−0.6
17	66.5	−10.7	75.7[h]	−1.3
18	72.1	−12.6	74.0[h]	−1.1
19	75.9[i]	−14.5	–	–
20	77.7[i]	−15.3	–	–

[a] Values $>>100$°C.
[b] L_{α}/Q_{II}.
[c] L_{α}/H_{II}.
[d] L_c/H_{II}.
[e] L_{β}/H_{II}.
[f] L_c/L_{β}.
[g] Q_{II}/L_{α}.
[h] H_{II}/L_{α}.
[i] H_{II}/L_{β}.

tive FTIR spectra for the lamellar crystalline, lamellar gel and lamellar liquid-crystalline (L_c, L_{β} and L_{α}, respectively) phases of di-15:0-β-GalDAG obtained on heating are shown in Fig. 5. In the CH_2 stretching region of the spectrum, there are only minor differences between the L_{β} and L_{α} phases. In the L_{α} phase, three strong bands are seen at 2956, 2922 and 2852 cm^{-1} and these narrow to give bands at 2954, 2917 and 2848 cm^{-1} in the L_{β} phase. The bands become slightly sharper in the L_c phase, but the frequencies remain the same. A 2 cm^{-1} shift in the CH_2 symmetric stretching band at 2851–2849 cm^{-1} is typical of transitions in which melted chains con-

Table 2
Low-angle X-ray diffraction spacings (cell lattice parameters, Å) of the phases observed in aqueous dispersions of some synthetic β-D-galactosyl diacylglycerols at specific temperatures (°C)

β-GalDAG	Phase				
	L_c	L_β	L_α	Q_{II}	H_{II}
10:0	38.8 (48.5)	45.9 (−6.8)	41.7 (69.4)	88.0[a] (84.7)	–
12:0	43.0 (63.5)	50.5 (23.1)	45.0 (58.5)	109.8[a] (78.8)	–
14:0	46.9 (68.7)	55.3 (44.2)	50.5 (48.1)	156.0[b] (73.8) 94.7[b]	–
15:0	50.3 (75.0)	58.0 (54.0)	52.8 (54.1)	171.4[c] (78.0)	–
16:0	51.4 (76.7)	60.8 (59.5)	54.4 (59.6)	159.6[d] (77.7)	72.5[d]
17:0	–	62.5 (64.0)	55.6 (68.0)	–	74.9 (76.0)
18:0	56.0 (81.7)	65.0 (66.5)	–[e]	–	77.5 (76.8)
19:0	–	66.9 (66.0)	–	–	79.9 (78.0)
20:0	60.0 (25)[f]	68.6 (71.5)	–	–	78.3 (76.7)

Note that the nonlamellar phases exhibit substantial hysteresis, so that the X-ray spacings may not represent equilibrium values (see Section 2).

[a] First order spacing of an unidentified phase. The possibility of multiple phases exists.

[b] This sample showed an $Im\bar{3}m/Pn\bar{3}m$ phase transition at ≈85°C.

[c] $Im\bar{3}m$.

[d] A mixture of cubic ($Im\bar{3}m$) and inverted hexagonal phases was evident in this lipid at elevated temperatures.

[e] The L_α phase only occurs over a very short temperature range in this lipid.

[f] A static measurement at 25°C.

vert to the ordered (all-*trans*) state (Lewis et al., 1990b).

On cooling in the CH_2 bending region at the L_α/L_β transition, there is practically no change in the frequency of the CH_2 scissoring band (≈1467 cm^{-1}), although the band does become narrower as the melted, liquid crystalline chains become ordered, gel phase chains. In the C = O stretching region, a single very broad band centered at ≈ 1735 cm^{-1} is visible in the L_α phase, which narrows to a band at ≈1740 cm^{-1} with a shoulder at ≈1720 cm^{-1} in the L_β phase.

These FTIR spectroscopic measurements confirm that the lower temperature thermal event, seen by DSC, corresponds to a chain-melting phase transition from a lamellar phase with ordered hexagonally packed chains, to one with melted hexagonally packed chains, i.e. an L_β (or L'_β)/L_α phase transition, in agreement with our earlier FTIR studies of the β-GlcDAGs (Lewis et al., 1990b).

The temperature and structural nature of the higher temperature thermal event seen in some samples by DSC is dependent on the direction of temperature change and on the lipid hydrocarbon chain length. At shorter chain lengths (10:0–13:0), the DSC measurements show that this transition may be supercooled by as much as 25°C on cooling. However, in some cases (notably when fast scan rates have been used to isolate these mesophases), the corresponding XRD measurements show that the higher temperature event is

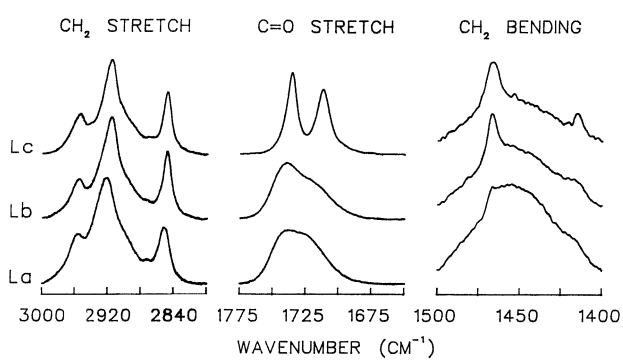

Fig. 5. Representative FTIR spectra of a sample of 1,2-di-*O*-pentadecanoyl-3-*O*-(β-D-galactopyranosyl)-*sn*-glycerol in the CH_2 stretch, C = O stretch and CH_2 bending regions in the L_c (top), L_β (middle) and L_α (bottom) phases.

not seen at the same temperature in DSC and XRD, probably reflecting the different scan rates characteristic of these techniques and the fact that this transition has a strong kinetic component. In these shorter chain compounds (10:0–13:0), there were insufficient X-ray reflections to identify the structure of these high temperature phases. At slightly longer chain lengths (14:0–16:0), the changes in the pattern of X-ray spacings across these higher temperature thermal events were consistent with L_α/inverted cubic phase transitions. However, in the di-14:0-β-GalDAG, the lamellar phase initially converts to a Q_{II} phase on heating, which has been tentatively identified as a double diamond cubic phase (space group $Pn\bar{3}m$). This phase is then gradually replaced by a second phase, tentatively identified as a plumber's nightmare cubic phase (space group $Im\bar{3}m$) at higher temperatures. The $Im\bar{3}m$ phase remains stable on cooling to ≈ 55°C, when it reverts to the $Pn\bar{3}m$ phase before becoming lamellar at ≈ 47°C. A similar pattern of behaviour exists in the di-15:0-β-GalDAG. At a chain-length of 16 carbon atoms, the phase seen on heating above ≈ 75°C consists of a mixture of Q_{II} (spacegroup $Im\bar{3}m$) and H_{II} phases (Fig. 4). Subsequently, the H_{II} phase disappears on cooling below ≈ 75°C, whereas the $Im\bar{3}m$ cubic phase is supercooled to ≈ 57°C, when it converts directly to the L_β phase. At longer chain lengths, in the di-17:0- and di-18:0-β-GalDAGs, the pattern of thermal events seen by DSC and the nature of the phase transitions seen on both heating and cooling simplifies. The DSC cooling curves show a single, sharp, weakly energetic exothermic event at higher temperature followed by a highly energetic exothermic event at slightly lower temperature. Immediate reheating shows that both of these transitions are reversible. Corresponding XRD measurements identify the lower temperature phase transition as an L_β/L_α phase transition and show a pattern of spacings characteristic of an H_{II} phase at high temperature. This identifies the higher temperature phase transition in these two chain-lengths as a L_α/H_{II} phase transition. The L_α/H_{II} phase transition does not exhibit hysteresis on cooling. FTIR measurements confirm the structure of the lamellar phases in the di-18:0 compound, which exhibits spectra identical to those found in the di-15:0-β-GalDAG shown in Fig. 5. These measurements show that the temperature window in which the L_α phase is stable decreases from 10.2°C in the di-17:0 compound to 2.5°C in the di-18:0 compound. At still longer chain lengths (di-19:0 and di-20:0-β-GalDAGs), only a single sharp peak is seen in both the heating and cooling curves by DSC, which corresponds to the L_β/H_{II} phase transitions visible in the XRD temperature profiles (Figs. 3 and 4).

3.3. Stable lamellar crystalline phase region

On nucleation at temperatures below the chain-melting phase transition, the L_β phases of these β-GalDAGs rapidly form an additional phase after an additional period of storage. DSC thermograms of suitably annealed samples show highly energetic endotherms on reheating. These events occur at significantly higher temperatures and have significantly higher enthalpy values than the equivalent L_β/L_α phase transitions (Fig. 3 and Table 1). Corresponding X-ray measurements of this stable phase show a pattern of spacings that is also characteristic of a lamellar phase. The conversion from the L_β phase to this new stable lamellar (L_c) phase is accompanied by a characteristic decrease in the lamellar repeat on storage at lower temperatures. XRD measurements clearly show that the nature of the L_c/lamellar liquid-crystalline phase transitions changes with increasing chain length (Fig. 4). At very short chain lengths, these transitions correspond to L_c/L_α phase transitions, whereas the di-12:0- to 16:0-βGalDAGs exhibit L_c/Q_{II} type transitions. At longer chain lengths, the di-17:0- to 20:0-β-GalDAGs exhibit L_c/H_{II} phase transitions. These differences reflect the change in the nature of the liquid-crystalline phase at high temperatures in this series of β-GalDAGs. In annealed samples of the di-10:0 species, an additional high temperature thermal event is observed between the L_β/L_α and L_c/L_α phase transitions at ≈ 48°C, which may correspond to the chain-melting transition of an L_c-type intermediate, as was observed in our earlier FTIR studies of the di-12:0-β-GlcDAG compound (Lewis et al., 1990b). In the

di-10:0-β-GalDAG studied here, the intermediate L_c phase can be converted to the more stable L_c phase by annealing the sample at 50°C. On subsequent reheating, the intermediate L_c/L_α phase transition is absent and the endothermic event attributed to the more stable L_c/L_α phase transition shows a proportionate increase in area.

In a earlier report, a semisynthetic di-stearoyl-β-GalDAGs derivative, prepared by catalytic hydrogenation of the di-linolenoyl species isolated from natural sources, was shown to undergo an exothermic event on heating following storage at 4°C for ≈ 24 h (Sen et al., 1983; Lis and Quinn, 1986; Quinn and Lis, 1987). DSC traces of samples of our synthetic di-18:0 and di-20:0-β-GalDAGs annealed in the above manner exhibited a transition containing both endothermic and exothermic components at temperatures below the L_c/H_{II} transition(s) on heating. The former event was previously thought to originate from a transition between a second low temperature crystalline phase (L_{c2}) formed after low temperature annealing and the stable crystalline phase (L_{c1}), initially formed following annealing at 22°C. Numerous attempts to induce this phase to form in samples of our synthetic di-16:0, 17:0 and 19:0-β-GalDAGs were unsuccessful, suggesting that long even-numbered chains may be required for the formation of this second lamellar crystalline phase. XRD measurements in the small-angle region revealed that the L_β to L_{c1} conversion process was accompanied by a significant decrease in d-spacing, but found no differences in the diffraction pattern of samples of our synthetic di-18:0 and di-20:0-β-GalDAGs annealed at 22°C and those further annealed at 0–4°C. Measurements of similarly annealed samples in the wide-angle region were not performed. FTIR measurements of the L_c phases formed in samples of the di-14:0-, di-15:0- and di-18:0-β-GalDAGs all show that the CH_2 stretching bands seen in the L_β phase at 2954, 2917 and 2848 cm^{-1}, become slightly sharper in the L_c phase, but the frequencies do not change. In the CH_2 bending region, the band at 1467 cm^{-1} becomes broader and is shifted to 1469 cm^{-1}, suggesting that more than one component may be present. The absence of the band seen at 1436 cm^{-1}, as well as the factor group splitting visible in the L_{c2} phase of the β-GlcDAGs, probably indicates the existence of an orthorhombic hydrocarbon chain subcell in which the chains are close to being parallel (Lewis et al., 1990b). At the same time, a band at ≈ 1415 cm^{-1}, which can be attributed to the αCH_2 groups, becomes sharper, indicating that the packing in the interfacial region is more ordered.

In the C = O stretching region, the narrow band at ≈ 1740 cm^{-1} and the shoulder at ≈ 1720 cm^{-1} in the L_β phase are replaced by two sharp bands at 1736 and 1712 cm^{-1} in the L_c phase, which resemble those found in the intermediate L_{c1} phase of the β-GlcDAGs (Lewis et al., 1990b). The band at 1712 cm^{-1} is indicative of a strongly H-bonded carbonyl group, although it is not possible to say whether this band arises from the *sn*-1 or *sn*-2 acyl chain.

Additional FTIR spectra of lipids subjected to annealing protocols used to form the L_{c2} phase were also performed, but on the time scale of the DSC experiment there were no clear differences in the spectra of lipids annealed at 22°C and those further annealed at 4°C. Thus, the exact nature of the structural difference between the L_{c1} and L_{c2} phases in the di-18:0 and di-20:0-β-GalDAGs remains unclear at this time.

3.4. Calculated thermodynamic and structural parameters

The temperatures and enthalpy changes associated with the thermotropic transitions of the β-GalDAGs are listed in Table 1. The L_β/L_α transition temperatures and associated enthalpy changes are strongly chain length-dependent and when plotted as a function of acyl chain length (Fig. 6), both parameters show relatively smooth monotonic increases with acyl chain length without any discontinuities between the odd- and even-numbered homologues. This is generally what is expected of simple chain-melting phenomena, in which the melted phase (in this case the L_α phase) is nucleated from a loose, hexagonally packed structure (Broadhurst, 1962). However, a close inspection of Fig. 6 shows that the enthalpy values for the di-19:0 and di-20:0 compounds are slightly higher than extrapolated from the trends

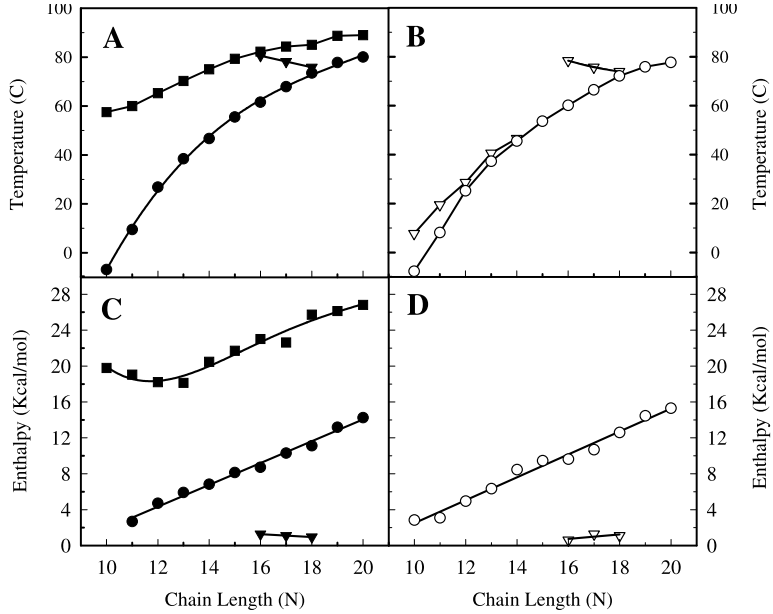

Fig. 6. Plots of the transition temperatures and enthalpies as a function of chain length for a series of 1,2-di-*O*-acyl-3-*O*-(β-D-galactopyranosyl)-*sn*-glycerols. The symbols are as follows: circles, L_β/L_α and L_α/L_β; squares, L_c/L_α; triangles, L_α/NL and NL/L_α; filled = heating; hollow = cooling.

set by the shorter chain homologues. This probably results from the fact that the enthalpy change measured for the two long chain compounds contains a small additional contribution (expected range 1.5–2 Kcal/mol) for the conversion of the L_β phase directly to the H_{II} phase. The chain length dependence of the lamellar liquid-crystalline to nonlamellar phase is not as straightforward because the nature of the nonlamellar phase formed is itself chain length dependent. Nevertheless, it is clear that the temperatures at which the L_α phases of these lipids become unstable with respect to an inverted nonlamellar phase decrease as the length of the acyl chains increases.

Also illustrated in Fig. 6 are plots of the chain length dependence of the transition temperatures and associated enthalpy changes of the phase transitions from each L_c phase in these glycolipids. There are no distinct odd/even discontinuities in the chain length dependence of the observed L_c/liquid crystalline phase transition temperatures and associated enthalpy values. Odd–even alternation, which was a feature of the L_c phase transition temperatures of both the β- and α-GlcDAGs (Mannock et al., 1988, 1990a; Sen et al., 1990), is believed to originate from the formation of a strongly hydrocarbon chain-tilted, lamellar crystal-like phase (Broadhurst, 1962). A plot of the lamellar repeats for the β-GalDAGs is shown in Fig. 7. The regression lines for the L_β

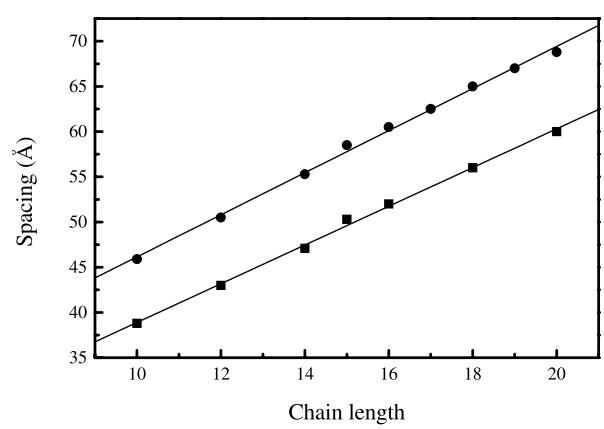

Fig. 7. Lamellar repeats (Å) of the L_β (●) and L_c (■) phases of the 1,2-di-*O*-acyl-3-*O*-(β-D-galactopyranoside)-*sn*-glycerols, plotted as a function of chain length. The data were taken from Table 2.

and L_c phases, which were calculated using the procedure outlined by Sen et al. (1990), have similar slopes but different intersects on the *y*-axis (L_β ●, 0.233, 2.286; L_c ■, 0.214, 1.748.). A slope of 0.233 for the L_β phases corresponds to a tilt angle of 24.5°, whereas the slope of the regression line for the L_c phases of 0.214 corresponds to a tilt angle of 33°. Both of these values are less than those of 31° and 35°, respectively, reported for the α-GlcDAGs (Mannock et al., 1990b; Sen et al., 1990). In the case of the β-GalDAGs, the linearity of the L_c phase transition temperatures, enthalpies (except at very short chain lengths where stronger headgroup hydrogen bonding interactions may be responsible for a small increase in enthalpy) and lamellar repeats suggests that the structure of the L_c phases is invariant with chain length and thus that the L_c phases are isostructural. This idea is further supported by the FTIR measurements of the di-14:0-, 15:0- and 18:0-β-GalDAGs, which show very similar L_c phase spectra.

4. Discussion

4.1. Mesophase region

The *n*-saturated 1,2-diacyl-3-*O*-(β-D-galactopyranosyl)-*sn*-glycerols exhibit a rich pattern of phase polymorphism which is dominated by transitions involving the L_c and inverted nonlamellar liquid-crystalline phases. The typical pattern of metastable mesophase events consists of a moderately energetic, lower temperature, metastable L_β/L_α phase transition with a higher temperature, weakly energetic L/NL phase transition. On cooling, the L_β/L_α phase transition is reversible and its temperature and enthalpy vary as a function of chain length, the former describing a smooth curve, whereas the latter increases linearly as expected of a simple chain-melting process (Fig. 6).

A comparison of the L_β/L_α phase transition temperatures of the β-GalDAGs with those of other NL phase-preferring lipids (Table 3) shows that they are similar to those of the diacyl PEs, but are higher than those of both the α- and β-GlcDAGs. Yet from a structural perspective, the lamellar repeats of the L_β and L_α phases of the β-GalDAGs, α-GlcDAGs and β-GlcDAGs of equivalent chain-length is very similar (Table 4). The last result is not surprising because any differences in the total length of the above glycolipids would be extremely small. Nevertheless, the similarity in the XRD d-spacings does not mean that all of the physical parameters within those bilayers are identical. We have already discussed the differences in the entropy across the L_β/L_α phase transition of several glycolipids in an earlier paper (Mannock et al., 1990b). Such thermodynamic parameters are likely to reflect relative differences in the tightness of the molecular packing in these lamellar phases. Indeed, the higher L_β/L_α phase transition temperatures of the β-GalDAGs relative to the other lipids listed in Table 3 must originate from the tighter molecular packing arising from the strong headgroup–headgroup interactions in the L_β phases of the β-GalDAGs. Such relative differences in order might be expected to manifest themselves as differences in the elasticity/compressibility of similar phases.

With increasing temperature, the lamellar phases become unstable and nonlamellar phases are formed. In the short (di-10:0-13:0) and medium (di-14:0–16:0) chain compounds, Q_{II} phases are initially formed above the chain-melting phase transition, as has been previously observed in the α- and β-GlcDAGs (Mannock et al., 1988, 1990b). At very short chain-lengths (di-10:0–12:0), a cubic phase exists at high temperature which we have been unable to identify by XRD. In the medium chain compounds, such as the di-14:0-β-GalDAG, regions with diffraction patterns characteristic of $Im\bar{3}m$ and $Pn\bar{3}m$ phases are visible on heating and cooling. The heating profile is dominated by $Im\bar{3}m$, whereas the cooling profile is dominated by $Pn\bar{3}m$ (Figs. 3 and 4) in a manner which is reminiscent of the hysteresis seen in the cubic phase region of the didodecyl-β-D-GlcDAGs (Mannock et al., 1992; Turner et al., 1992). Thus, the cubic phase region of the phase diagram of these β-GalDAGs is more complicated than that in either the α- or β-GlcDAGs (Mannock et al., 1988, 1990b) in that more than one type of Q_{II} phase is observed. This $Im\bar{3}m/Pn\bar{3}m$ combination of cubic phases has also been observed in studies of shorter chain dialkyl PEs

Table 3
Thermodynamic properties of the various phase transitions of the glycosyl diacylglycerols and phosphatidylethanolamines dispersed in excess water

Acyl chain length	β-D-Gal		α-D-Glc		β-D-Glc		PE	
	T_m	ΔH	T_m	ΔH	T_m	ΔH	T_m	ΔH
[9]*(A) The lamellar/inverted nonlamellar phase transition*								
12	[a]	–	[a]	–	57.8[b]	0.3	[a]	–
13	[a]	–	[a]	–	59.0	0.3	[a]	–
14	80.6	0.4	105.0[c]	0.3	72.0[b]	0.8	[a]	–
15	≈75	–	82.0	0.4	73.4	0.7	–	–
16	80.7[b] [c]	1.3	79.1[b]	1.1	75.0[c]	1.5	123.0[c]	0.3
17	78.1[c]	1.1	76.6[c]	1.4	73.9[c]	1.5	–	–
18	76.0[c]	1.0	74.5[c]	1.0	73.8[c]	1.1	101.0[c]	0.9
19	77.8[d]	13.2	73.7[d]	14.4	76.5[d]	13.3	–	–
20	80.0[d]	14.25	76.8[d]	15.4	79.7[d]	14.7	96.0[c]	0.8
(B) The metastable gel chain-melting phase transition								
10	−6.9	–	–	–	–	–	2.0	1.8
11	9.5	2.7	1.9	3.7	–	–	–	–
12	26.8	4.7	19.5	5.8	26.0	4.9	30.5	3.7
13	38.5	5.9	32.9	6.1	35.7	5.8	–	–
14	48.7	6.8	40.5	7.4	45.5	6.7	50.5	5.6
15	55.5	8.1	50.7	8.9	54.2	8.2	–	–
16	61.6	8.7	57.2	9.5	61.0	9.0	64.4	7.9
	55.4[e]	6.0						
17	67.9	10.3	63.4	10.4	67.0	10.2	–	–
18	73.5	11.1	68.4	12.2	71.7	11.2	73.5	10.5
	73.3[e]	7.4						
19	77.8[d]	13.2	73.7[d]	14.4	76.5[d]	13.3	–	–
20	80.0[e]	14.3	76.8[e]	15.4	79.7[e]	14.7	82.0	12.5
(C) The stable gel phase transition								
10	57.5	19.8	31.1	21.0	–	–	26.6	11.9
11	60.0	19.0	29.4	14.2	–	–	–	–
12	65.3	18.2	45.9	18.5	38.6	14.3	44.5	13.3
13	70.3	18.1	46.7	18.5	45.8	16.3	–	–
14	75.4	20.7	58.2	21.2	46.5	18.3	57.0	14.8
15	79.3	21.7	56.7	21.2	54.8	18.0	–	–
16	82.3[f]	23.0	66.1	23.6	56.2[g]	14.0	64.9	18.5
	74.4[e]	14.3						
17	84.3[f]	22.6	66.8	21.7	63.1[g]	9.1	–	–
18	85.0[f]	25.7	73.9[f]	29.0	58.1[g]	8.8	–	–
	88.5[e]	16.0						
19	88.7[f]	26.1	59.9[g]	6.6	–	–	–	–
20	89.0[f]	26.8	78.9[f]	31.8	62.5[g]	10.8	–	–

Data were obtained from the following Refs.: Mannock et al. (1988), Mannock et al. (1990b), Seddon et al. (1983), Singer et al. (1990) and Mantsch et al. (1983).

[a] Values $>>100$°C or could not be resolved by the Perlin-Elmer DSC.

[b] L_α/Q_{II} transitions.

[c] L_α/H_{II} transitions.

[d] L_β/H_{II} transitions.

[e] Semisynthetic β-Gal DAGs calculated from Refs. Sen et al. (1983), Mannock (1984) and Mannock et al. (1985).

[f] L_c/H_{II} transitions.

[g] L_c/L_β transitions.

Table 4
Small-angle X-ray diffraction spacings (cell lattice parameters, Å) of the phases observed in some synthetic α- and β-D-glycosyl diacylglycerols dispersed in excess water

Head group	Chain length	Phase				
		L_c	L_β	L_α	Q_{II}	H_{II}
α-Glc[a]	14:0	41.5	53.5	50.0	101.0	–
	16:0	45.5	59.0	–	112.0	–
β-Glc[b]	14:0	47.8	53.5	49.8	91.0	–
	16:0	51.6	60.3	52.9	–	65.8
β-Gal	14:0	46.9	55.3	50.5	156.0[c]	–
	16:0	51.4	60.8	54.4	159.6[d]	72.5

Note that the nonlamellar phases exhibit substantial hysteresis, so that the X-ray spacings may not represent equilibrium values (see Section 2).
[a] Sen et al. (1990).
[b] Mannock et al. (1988).
[c] This sample showed an $Im\bar{3}m/Pn\bar{3}m$ phase transition at $\approx 85°C$.
[d] A mixture of cubic ($Im\bar{3}m$) and inverted hexagonal phases was evident in this lipid at elevated temperatures.

(Seddon et al., 1990; Seddon, 1990) and dialkyl-β-GalDAGs (Kuttenreich et al., 1988, 1993; Tenchova et al. 1996), whereas the $Ia\bar{3}d$/ $Pn\bar{3}m$ combination appears to be preferred in the dialkyl-β-D-GlcDAGs (Turner et al., 1992), presumably reflecting subtle differences in headgroup interactions in these compounds. It is also interesting that the nonlamellar preference has a similar chain length dependence to that observed in the β-GlcDAGs (Mannock et al., 1988).

At still higher temperatures (75–80°C) and longer chain-lengths (di-16:0–18:0), the Q_{II} phase becomes energetically unfavorable and is replaced in the nonlamellar phase region by the H_{II} phase. Although it is interesting that in the di-16:0-β-GalDAG a region of Q_{II}/H_{II} phase coexistence is observed, in the di-17:0- and 18:0-β-GalDAGs, the L/NL event is a discrete L_α/H_{II} phase transition. The fact that both Q_{II} and H_{II} phases are formed in the di-16:0-β-GalDAG suggests that these compounds are closer in their NL phase propensity to the β-GlcDAGs than the α-anomers, where the H_{II} phase is only seen at longer chain lengths ($\geq$17:0). Concurrent with this change in NL phase structure, the temperature interval between the L_β/L_α and L/NL phase transitions decreases with increasing chain length until, in both di-19:0 and 20:0-β-GalDAGs, no L_α phase is evident and L_β/H_{II} phase transitions occur. L_β/H_{II} phase transitions are typical of most NL preferring lipids with long chains (Table 3).

The phase transition temperatures obtained for the pure synthetic β-GalDAGs shown in Table 1 are in good agreement with earlier reports for the semi-synthetic di-16:0- and di-18:0-β-GalDAGs (Sen et al., 1983; Mannock et al., 1985). The minor differences between the transition temperatures and enthalpy values reported here and those for the semisynthetic lipids (Sen et al., 1983; Mannock et al., 1985) most likely originate from errors introduced from manual estimation of the baseline under the phase transition peak and the acyl chain heterogeneity of the compounds used in the earlier studies.

The L_α/H_{II} phase transition temperatures of the β-GalDAGs (Table 3) are considerably lower than those of the diacyl PEs, slightly higher than those of the α-GlcDAGs and higher still than those of the corresponding β-GlcDAGs. The similarity of the X-ray first-order spacings for the L_α phases of aqueous dispersions of the β-GalDAGs and α- and β-GlcDAGs (Mannock et al., 1988; Sen et al., 1990) suggests that variations in headgroup size in these nonionic glycolipids does not appreciably alter the overall structure or dimensions of the L_α phase. However, the headgroup dependence of the

thermal stability of this L_α phase and the variation in the headgroup dependence of the nonlamellar phase formed in compounds with the same hydrocarbon chain length, implies that the headgroup does play a limiting role in the formation of nonlamellar phases. One possible scenario that would explain this behavior arises if the headgroups have different abilities to counteract the dynamic volume of the hydrocarbon chains at the L/NL phase transition. This suggestion is supported by studies on the dialkyl glycolipids from our collaborators (Duesing et al., 1997; Seddon et al., 1996) and from those of Hinz's group (Hinz et al., 1991; Koynova et al., 1993; Kuttenreich et al., 1993), which show that the chain-melting phase transition temperature only changes by a very small amount on altering the nature of the single nonionic glycopyranoside headgroup, while both the temperature of the L/NL phase transition and the associated structural changes may be dramatically altered. Model calculations, based on Fourier reconstructions of some small-angle X-ray measurements of several nonlamellar-preferring phospho- and glycolipid membranes at their respective L_α/H_{II} phase transitions, suggest a similar interpretation (Lewis et al., 1989, 1990a; Harper et al., 2001; Mannock et al., 2001).

4.2. Crystalline phases

Upon nucleation at suitable temperatures and annealing at 22°C for 2–3 days, the L_β phases present in all the β-GalDAGs are converted to more stable L_c phases, which undergo very energetic, high-temperature, chain-melting transitions on heating to one of three types of liquid-crystalline phase depending on their hydrocarbon chain length. Lipids with 13 carbon chains or less convert to the L_α phase, whereas lipids with 14 or 15 carbon chains convert directly to a Q_{II} phase. At a chain-length of 16 carbon atoms or longer, the L_c phase converts to a Q_{II}/H_{II} phase mixture. The transition temperatures for the L_c/liquid-crystalline phase transition of the di-16:0- and di-18:0-β-GalDAGs are in reasonable agreement with earlier reports for semi-synthetic materials of similar chain-length (Sen et al. 1983; Mannock et al., 1985; Lis and Quinn, 1986; Quinn and Lis, 1987). The discrepancies visible in the sets of transition temperatures listed for the pure and semi-synthetic di-16:0-β-GalDAG reflect the presence of positional isomers containing both 14 and 18 carbon fatty acids.

Apart from the intermediate L_c phase seen in the di-10:0-β-GalDAG, which we have not been able to isolate in pure form for the purpose of making measurements (Mannock and McElhaney, 1991), all of the stable L_c phases formed in the β-GalDAGs appear to be isostructural, as determined by low-angle XRD and FTIR spectroscopy. The only deviation in the available data seems to be at short chain lengths, where the enthalpy values for the L_c/L_α phase transitions in the di-10:0 to 12:0-β-GalDAGs are greater than would be expected. This may reflect a small change in the balance of headgroup versus hydrocarbon chain packing contributions at short versus long chain lengths, as we have previously suggested for the α-GlcDAGs (Sen et al., 1990).

The fact that the L_c/liquid-crystalline phase transition temperatures for the β-GalDAGs are higher than those reported for both the diacyl PEs (Mantsch et al. 1983; Singer et al. 1990) and the α- and β-GlcDAGs (Table 3) suggests that the L_c phases of the β-GalDAGs are very strongly hydrogen-bonded. This observation is supported by the very large enthalpy values associated with these events and has been confirmed by our own FTIR spectroscopy measurements, which show that the single narrow carbonyl band at 1740 cm^{-1}, which is typical of the L_β phase, is changed to two sharp bands at 1736 and 1712 cm^{-1} on conversion to the L_c phase. This pattern of behaviour closely resembles that seen in the L_{c1} phases of the corresponding β-GlcDAGs (Lewis et al., 1990b). The sharpening of the CH_2 scissoring bands at 1469 cm^{-1} and the absence of a band at 1436 cm^{-1} suggests that the hydrocarbon chains are packed in a parallel, all-*trans* configuration.

A comparison of the first-order spacings obtained using XRD for the L_c phases of the α-GlcDAGs shows that they are smaller than those of the β-GalDAGs (c.f. Figs. 2 and 7 of Sen et al., 1990) and β-GlcDAGs (Mannock et al., 1988) by some 6 Å (Table 4). The differences in the first

order spacings of the L_c phases cannot be directly attributed to a single factor, such as a difference in the headgroup 'size' or orientation. Simple calculations of the molecular dimensions (a single hexopyranoside has an O1–O4 distance of 4.2–4.6 Å; French et al., 1990) and an examination of space filling models shows that the differences in headgroup area (not allowing for water of hydration) between these three glycolipid configurations are relatively small. Even if the headgroups were to adopt extreme and energetically unfavorable conformations, the area per molecule would not change substantially, assuming that the hydrocarbon chains are perpendicular to the bilayer surface. This conclusion is also supported by the similarity of the first order spacings from the corresponding L_β phases (Table 4). If, under the circumstances described above, the hydrocarbon chains determined the area per molecule, then two other physical explanations of these differences in L_c phase first order spacings become possible, namely, differences in hydrocarbon chain tilt and differences in headgroup and/or hydrocarbon chain interdigitation. A comparison of the plot of lamellar repeats for the L_c phases for the β-GalDAGs shown in Fig. 7 with that of α-GlcDAGs (Sen et al., 1990) (there is insufficient XRD data from our earlier studies of the β-GlcDAGs to include them in this comparison) shows that the L_c phase tilt angle (33°) of the β-GalDAGs is less steep than that of the α-GlcDAGs (35°). Thus, there is a difference in the tilt angle of the respective L_c phases. However, it is still insufficient to account for the considerable difference (6 Å) in the thickness of the L_c phase bilayer in the α-GlcDAGs versus the β-GalDAGs and β-GlcDAGs. The most likely explanation for this structural difference is that the L_c phase of the α-GlcDAGs is interdigitated, whereas that of the β-GalDAGs is not. At this time, however, we are unable to say whether this interdigitation in the α-GlcDAGs involves the headgroup or hydrocarbon chain regions or both (Sen et al., 1990).

While the structure of the L_c phases of the odd and even chain β-GalDAGs appears to be similar, the kinetics of the L_β/L_c conversion process show significant odd/even alternation, the odd chain compounds being slower to convert than the even chain compounds. Despite this, the odd/even alternation in the transition temperatures involving the L_c phases of both the α-GlcDAGs and β-GlcDAGs is absent. Whether this reflects a difference in the hydrocarbon chain packing (parallel versus perpendicular) in the L_c phases formed in these β-GalDAGs is not presently clear (Lewis et al., 1990b).

In addition, the difference in the rate of conversion between the odd and even chain compounds is not as great as that reported for either the α- or the β-GlcDAGs (Mannock et al., 1988, 1990b; Lewis et al., 1990b). Even chain compounds always convert faster than the odd chain lipids in all three systems. Upon initial inspection, in the absence of chain length effects, the following relationships are evident for the kinetics of the crystallization path:[3]

$$\begin{array}{ccccc} \text{even-β-GalDAG} \geq \text{even-α-GlcDAG} > > \text{even-β-GlcDAG}(L_{c1}) & & & & \vee \\ \vee & & \vee & & \vee \\ & & \vee & & \vee \\ \text{odd-β-GalDAG} > > > \text{odd-α-GlcDAG} > > > \text{odd-β-GlcDAG} & & & & \end{array}$$

At a fundamental level, this combination of odd/even alternation in phase transition temperature and differences of the kinetics of the phase transformation must arise from differences in chain tilt and chain and headgroup interdigitation (Mannock et al., 1988, 1990b; Sen et al., 1990; Lewis et al., 1990b), but the problem is a complex one in which no single determinant has been definitively identified as the causal factor. In the β-GalDAGs studied here, the existence of an isostructural L_c phase, in which the chains are in an all-*trans* configuration parallel to the zigzag planes, argues for the influence of end group

[3] The symbols '>' (greater than), '?' (greater than or equal to) and '?' (an inverted caret symbol, representing a greater than or equal to symbol rotated by 90°) are an indication of the rate of change of the L_γ/L_c phase conversion process in this two dimensional scheme. The more symbols that are present, the greater the difference in rates.

effects in the odd/even phase conversion process. In such a scenario, the odd and even numbered chain termini would differ in their ability to pack in the desired L_c phase minimum energy conformation. Another contributing factor to the kinetics of the crystallization path must be the ability of the hydrocarbon chains to reorganize to form a different chain subcell, for example, in the conversion from L_{c1} to L_{c2} in the β-GlcDAGs, where the chains reorient from a parallel to a perpendicular conformation at shorter chain-lengths to favor stronger hydrogen bonds with the headgroup (Lewis et al., 1990b; Mannock et al., 1992; Mannock et al., 1994). The chain length dependence of this reorganization and the fact that it is not present in all of the above glycolipids, suggests that there must also be a headgroup component directing this process. The headgroup component in this equation should not be overlooked, as it is likely that the balance between solvent–solute and solute–solute hydrogen-bonding interactions and the orientation of those bonds in space determines the structure of the L_c phase. The chains regulate the rate at which these events can occur and what chain packings are possible. Interdigitation arises from a combination of these events.

In conclusion, while there are clearly differences in the thermotropic phase properties of the βGalDAGs studied here with those of other nonlamellar preferring phospho- and glycolipids (Table 3), the accumulating evidence seems to suggest that, for lipids of the same chain length, motional averaging results in lamellar mesophases with similar structural dimensions which may differ slightly in some of their headgroup dependent surface and bulk properties, which in turn affect the thermodynamic stability of those mesophases. Our observations suggest that there are two competing sets of interactions which may explain the patterns of phase behaviour seen in these lipids; (1) that the headgroup interactions regulate both the hydrogen-bonding networks and hydration at the bilayer surface and consequently determine the hydrocarbon chain packing within the bilayer and thus, the structure of the L_c phase; and (2) that it is the collective properties of the headgroup (the nature, number and strength of the interactions between neighboring lipid molecules as well as those with water) and its ability to counterbalance the increasing dynamic volume of the hydrocarbon chains which determines the nonlamellar phase behavior of these lipids. Such a hypothesis may account for the differences in both the L/NL and solid-state polymorphism which have recently been observed in lipid molecules with similar chemical structures which differ only in their chirality of the glycerol backbone (Mannock et al., 1991), as well as those containing pentopyranosides (Seddon et al., 1996; Duesing et al., 1997). Thus, the emerging picture is one in which the most significant differences in the phase properties of these lipids exist under circumstances in which the lipids are closely packed in the headgroup region, i.e. in the formation of L_c and nonlamellar phases. At this time, what remains to be determined are the mechanical details regulating both the L_β/L_c phase conversion process and those of the L/NL phase transitions. Such studies are presently underway in our respective laboratories.

Acknowledgements

This work was supported by grants from the Canadian Institute for Health and Research and the Alberta Heritage Foundation for Medical Research to RNM and by grants from the National Institutes of Health (GM32614) and Department of Energy (DE-FGO287ER60522) to SMG. PEH was supported by fellowships from the National Science Foundation and the Liposome Company. We would also like to thank Professor J. Diakur (University of Alberta, Pharmacy) and Professor M. Kates (University of Ottawa, Biochemistry) for their assistance in obtaining ^{1}H-NMR date.

References

Azuma, M., Kato, K., Ikarashi, Y., Asada-Mikami, R., Maruoka, H., Takaue, Y., Saito, A., Wakasugi, H., 2000. Cytokines production of U5A2-13-positive T cells by stimulation with glycolipid alpha-galactosylceramide. Eur. J. Immunol. 30, 2138–2146.

Bashkatova, A.I., Smirnova, G.V., Volynskaya, V.N., Shvets, V.I., Evstigneeva, R.P., 1973. Investigations in the field of glycosyldiglycerides V. Synthesis of galactosyl diglyceride. Zh. Org. Khim. 9, 1422–1429.

Batrakov, S.G., Il'ina, E.F., Panosyan, A.G., 1976. Synthesis of monoglycosyl diglycerides and their derivatives. Izvest. Akad. Nauk. SSSR Ser. Khim. 3, 626–632.

Bhat, S., Spitalnik, S.L., Gonzalez-Scarano, F., Silberberg, D.H. 1991. Galactosyl ceramide or a derivative is an essential component of the neural receptor for human immunodeficiency virus type 1 envelope glycoprotein gp 120. Proceedings of the National Academy of Sciences of the United States of America. 88 (16): 7131–4.

Broadhurst, M.G. 1962. An analysis of the solid state behavior of normal paraffins. J. Res. Natl. Bureau Stand. 66A: 241–249.

Brogi, A., Presentini, R., Piomboni, P., Collodel, G., Strazza, M., Solazzo, D., Costantino-Ceccarini, E., 1995. Human sperm and spermatogonia express a galactoglycerolipid which interacts with gp120. J. Submicrosc. Cytol. Pathol. 27, 565–571.

Brogi, A., Presentini, R., Solazzo, D., Piomboni, P., Costantino-Ceccarini, E., 1996. Interaction of human immunodeficiency virus type 1 envelope glycoprotein gp120 with a galactoglycerolipid associated with human sperm. AIDS Res. Hum. Retro. 6, 483–489.

Brogi, A., Presentini, R., Moretti, E., Strazza, M., Piomboni, P., Costantino-Ceccarini, E., 1998. New insights into the interaction between the gp120 and the HIV receptor in human sperm. J. Reprod. Immunol. 41, 213–231.

Duesing, P.M., Seddon, J.M., Templer, R.H., Mannock, D.A., 1997. Pressure effects on lamellar and inverse curved phases of fully hydrated dialkyl phosphatidylethanolamines and β-D-xylopyranosyl-*sn*-glycerols. Langmuir 13, 2655–2664.

French, A.D., Rowland, R.S., Allinger, N.L., 1990. Modeling of glucopyranose. In: French, A.D., Brady, J.W. (Eds.), Computer Modeling of Carbohydrate Molecules. American Chemical Society, Washington, DC, pp. 120–140 ACS Symposium Series 430.

Gadella, B.M., Gadella, T.W.J., Colenbrander, B., van Golde, L.M.G., Lopes-Cardozo, M., 1994. Visualization and quantification of glycolipid polarity dynamics in the plasma membrane of the mammalian spermatozoon. J. Cell Sci. 107, 2151–2163.

Gadella, B.M., Hammache, D., Pieroni, G., Colenbrander, B., vanGolde, L.M.G., Fantini, J., 1998. Glycolipids as potential binding sites for HIV: topology in the sperm plasma membrane in relation to the regulation of membrane fusion. J. Reprod. Immunol. 41, 233–253.

Gent, P.A., Gigg, R., 1975. Synthesis of 1,2-di-*O*-hexadecanoyl-3-*O*-(β-D-galactopyranosyl)-L-glycerol (a 'galactosyl diglyceride') and 1,2-di-*O*-octadecanoyl-3-*O*-(6-*O*-octadecanoyl-β-D-galactopyranosyl)-L-glycerol. J. Chem. Soc. Perkin 1, 364–370.

Gonzalez-Aseguinolaza, G., de Oliveira, C., Tomaska, M., Hong, S., Bruna-Romero, O., Nakayama, T., Taniguchi, M., Bendelac, A., Van Kaer, L., Koezuka, Y., Tsuji, M., 2000. Alpha-galactosylceramide-activated v alpha 14 natural killer T cells mediate protection against murine malaria. Proc. Natl. Acad. Sci. USA 97, 8461–8466.

Guerrero, C.A., Zarate, S., Corkidi, G., Lopez, S., Arias, C.F. 2000. Biochemical characterization of rotavirus receptors in MA104 cells. J Virol. 74 (20): 9362–71.

Handa, K., Kojima, N., Hakomori, S.I. 2000. Analysis of glycolipid-dependent cell adhesion based on carbohydrate-carbohydrate interaction Methods Enzymol. 312: 447–58.

Hajduk, D.A., Harper, P.E., Gruner, S.M., Honeker, C.C., Kim, G., Thomas, E.L., Fetters, L.J., 1994. The gyroid: A new equilibrium morphology in weakly segregated diblock copolymers. Macromolecules 27, 4063–4075.

Harper, P.E., Mannock, D.A., Lewis, R.N.A.H., McElhaney, R.N., Gruner, S.M., 2001. X-ray determination and comparison of the molecular structure of some phosphatidylethanloamines in the lamellar and inverse hexagonal (H_{II}) phases. (Accepted by the Biophysical Journal).

Hinz, H.-J., Kuttenreich, H., Meyer, R., Renner, M., Fründ, R., 1991. Stereochemistry and size of sugar headgroups determine the structure and phase behavior of glucolipid membranes. Densitiometric, calorimetric and X-ray studies. Biochemistry 30, 5125–5138.

Kakimi, K., Guidotti, L.G., Koezuka, Y., Chisari, F.V., 2000. Natural killer T cell activation inhibits hepatitis B virus replication in vivo. J. Exp. Med. 192, 921–930.

Kaplun, A.P., Shvets, V.I., Evstigneeva, R.P., 1977. Investigations in the field of glycosyldiglycerides VI. A study of the glycosylation of glycerol derivatives by orthoesters and acylglycosylhalides of D-glucose and D-galactose. Bioorgan. Khim. 3, 222–231.

Kaplun, A.P., Shvets, V.I., Evstigneeva, R.P., 1978. Investigations in the field of glycosyldiglycerides VIII. Synthesis of natural 1,2-*trans*- and 1,2-*cis*-glycosyldiglycerides. Zh. Org. Khim. 14, 256–258.

Kitamura, H., Ohta, A., Sekimoto, M., Sato, M., Iwakabe, K., Nakui, M., Yahata, T., Meng, H., Koda, T., Nishimura, S., Kawano, T., Taniguchi, M., Nishimura, T., 2000. Alpha-galactosylceramide induces early B-cell activation through IL-4 production by NKT cells. Cell Immunol. 199, 37–42.

Koynova, R.D., Tenchov, B.G., Kuttenreich, H., Hinz, H.J., 1993. Structure and phase behavior of a charged glycolipid, (1,2-*O*-dialkyl-3-*O*-beta-D-glucuronosyl-*sn*-glycerol). Biochemistry 32, 12437–12445.

Kulkarni, K., Snyder, D.S., McIntosh, T.J. 1999. Adhesion between cerebroside bilayers. Biochemistry. 38 (46): 15264–71.

Kuttenreich, H., Hinz, H.-J., Inczedy-Marcsek, M., Koynova, R., Tenchov, B., Laggner, P., 1988. Polymorphism of synthetic 1,2-dialkyl-3-*O*-(β-D-galactosyl)-*sn*-glycerols of different alkyl chain lengths. Chem. Phys. Lip. 47, 245–260.

Kuttenreich, H., Hinz, H.-J., Koynova, R.D., Tenchov, B.G., 1993. Different phase behaviour of *sn*-1 and *sn*-3 stereoisomers of the glycolipid di-tetradecyl-(β-D-galactosyl)-glycerol. Chem. Phys. Lip. 66, 55–62.

Lewis, R.N.A.H., Mannock, D.A., McElhaney, R.N., Turner, D.C., Gruner, S.M., 1989. Effect of fatty acid chain length

and structure on the lamellar gel to liquid-crystalline and lamellar to reversed hexagonal phase transitions of aqueous phosphatidylethanolamine dispersions. Biochemistry 28, 541–548.

Lewis, R.N.A.H., Mannock, D.A., McElhaney, R.N., 1990a. Lamellar to nonlamellar phase transitions of phosphatidylethanolamines and monoglycosyl diacylglycerols. Zbl. Bakt. Suppl. 20, 643–645.

Lewis, R.N.A.H., Mannock, D.A., McElhaney, R.N., Wong, P.T.T., Mantsch, H.H., 1990b. The physical properties of glycosyl diacylglycerols. An infrared spectroscopic study of the gel phase polymorphism of the 1,2-di-*O*-acyl-3-*O*-(β-D-glucopyranosyl)-*sn*-glycerols. Biochemistry 29, 8933–8943.

Lingwood, C., Schramayr, S., Quinn, P., 1990. Male germ cell specific sulfogalactoglycerolipid is recognized and degraded by mycoplasmas associated with male infertility. J. Cell Physiol. 142, 170–176.

Lis, L.J., Quinn, P.J., 1986. A time resolved synchrotron X-ray study of a crystalline phase bilayer transition and packing in a saturated monogalactosyldiacylglycerol-water system. Biochim. Biophys. Acta 862, 81–86.

MacMurray, T.A., Morrison, W.R., 1970. Composition of wheat-flour lipids. J. Sci. Food Agric. 21, 520–528.

Mannock, D.A., 1984. The phase properties of galactolipids isolated from blue-green algae and higher plants. Ph.D. thesis. University of London, UK.

Mannock, D.A., Brain, A.P.R., Williams, W.P., 1985. The phase behaviour of 1,2-diacyl-3-monogalactosyl-*sn*-glycerol derivatives. Biochim. Biophys. Acta 817, 289–298.

Mannock, D.A., Lewis, R.N.A.H., McElhaney, R.N., 1987. An improved procedure for the preparation of 1,2-di-*O*-acyl-3-*O*-(β-D-glucopyranosyl)-*sn*-glycerols. Chem. Phys. Lip. 43, 113–127.

Mannock, D.A., Lewis, R.N.A.H., Sen, A., McElhaney, R.N., 1988. The physical properties of glycosyl diacylglycerols. Calorimetric studies of a homologous series of 1,2-di-*O*-acyl-3-O-(β-D-glucopyranosyl)-*sn*-glycerols. Biochemistry 27, 6852–6859.

Mannock, D.A., Lewis, R.N.A.H., McElhaney, R.N., 1990a. The chemical synthesis and physical characterization of 1,2-di-*O*-acyl-3-*O*-(α-D-glucopyranosyl)-*sn*-glycerols, an important class of membrane glycolipids. Chem. Phys. Lip. 55, 309–321.

Mannock, D.A., Lewis, R.N.A.H., McElhaney, R.N., 1990b. The physical properties of glycosyl diacylglycerols. 1. Calorimetric studies of a homologous series of 1,2-di-*O*-acyl-3-*O*-(α-D-glucopyranosyl)-*sn*-glycerols. Biochemistry 29, 7790–7799.

Mannock, D.A., McElhaney, R.N. 1991. Differential scanning calorimetry and X-ray diffraction studies of a series of synthetic β-D-galactosyl diacylglycerols. Biochem. Cell Biol. 69: 863–867.

Mannock, D.A., Lewis, R.N.A.H., McElhaney, R.N., Akiyama, M., Yamada, H., Turner, D.C., Gruner, S.M., 1992. The effect of chirality of the glycerol backbone on the bilayer and nonbilayer phase transitions in the diastereomers of di-dodecyl-β-D-glucopyranosyl glycerols. Biophys. J. 63, 1355–1368.

Mannock, D.A., McElhaney, R.N., Harper, P.E., Gruner, S.M. 1994. Differential scanning calorimetry and X-ray diffraction studies of the diastereomeric ditetradecyl β-D-galactosyl glycerols and their mixture. Biophys. J. 66: 734–740.

Mannock, D.A., Lewis, R.N.A.H., McElhaney, R.N., Harper, P.E., Gruner, S.M., 2001. Relationship between fatty acid composition and the lamellar gel to liquid crystalline and the lamellar to inverted nonlamellar phase transition temperatures of phosphatidylethanolamines and diacyl-α-D-glucosyl glycerols. (Accepted subject to revision the Biophysical Journal).

Mantsch, H.H., Hsi, S.C., Butler, K.W., Cameron, D.G., 1983. Studies on the thermotropic behaviour of aqueous phosphatidylethanolamines. Biochim. Biophys. Acta 728, 325–330.

Mantsch, H.H., Madec, C., Lewis, R.N.A.H., McElhaney, R.N., 1985. Thermotropic phase behaviour of model membranes composed of phosphatidylcholines containing iso-branched fatty acids. 2. Infrared and ^{31}P-NMR spectroscopic studies. Biochemistry 24, 2440–2446.

Nakata, K., 2000a. High resistance to oxygen radicals and heat is caused by a galactoglycerolipid in Microbacterium sp. M874. J. Biochem. (Tokyo) 127, 731–737.

Nakata, K., 2000b. Rescuing activity of galactoglycerolipids from cellular lesions induced by 5-aminolevulinic acid. J. Biochem. (Tokyo) 127, 813–819.

Nakata, K., Guo, C.T., Matsufuji, M., Yoshimoto, A., Inagaki, M., Higuchi, R., Suzuki, Y., 2000c. Influenza A virus-binding activity of glycoglycerolipids of aquatic bacteria. J. Biochem. (Tokyo) 127, 191–198.

Nishimura, T., Kitamura, H., Iwakabe, K., Yahata, T., Ohta, A., Sato, M., Takeda, K., Okumura, K., Van Kaer, L., Kawano, T., Taniguchi, M., Nakui, M., Sekimoto, M., Koda, T. 2000. The interface between innate and acquired immunity: glycolipid antigen presentation by CD1d-expressing dendritic cells to NKT cells induces the differentiation of antigen-specific cytotoxic T lymphocytes. Int Immunol. 12 (7): 987–94.

Nicol, A., Nieda, M., Koezuka, Y., Porcelli, S., Suzuki, K., Tadokoro, K., Durrant, S., Juji, T., 2000. Human invariant V alpha 24+ natural killer T cells activated by alpha-galactosylceramide (KRN7000) have cytotoxic anti-tumour activity through mechanisms distinct from T cells and natural killer cells. Immunology 99, 229–234.

Osman, Y., Kawamura, T., Naito, T., Takeda, K., Van Kaer, L., Okumura, K., Abo, T., 2000. Activation of hepatic NKT cells and subsequent liver injury following administration of alpha-galactosylceramide. Eur. J. Immunol. 30, 1919–1928.

Parks, J.E., Lynch, D.V., 1992. Lipid composition and thermotropic phase behaviour of boar, bull, stallion and rooster sperm membranes. Cryobiology 29, 255–266.

Quinn, P.J., Williams, W.P., 1983. The structural role of lipids in photosynthetic membranes. Biochim. Biophys. Acta 737, 223–226.

Quinn, P.J., Lis, L.J., 1987. Structural intermediates in phase transitions involving crystalline phase bilayers of monogalactosyldiacylglycerol in water. J. Coll. Interface Sci. 115, 220–224.

Ratledge, C., Wilkinson, S.G., (Eds.), 1988. Microbial Lipids, vol. 1. Academic Press, New York.

Reynolds, G.T., Milch, J.R., Gruner, S.M. 1978. A high sensitivity intensifier-TV detector for X-ray diffraction studies. Rev. Sci. Instr. 49: 1241–1249.

Sahasrabudhe, M.R., 1979. Lipid composition of oats (*Avena sativa* L.). J. Am. Oil Chem. Soc. 56, 80–84.

Saubermann, L.J., Beck, P., De Jong, Y.P., Pitman, R.S., Ryan, M.S., Kim, H.S., Exley, M., Snapper, S., Balk, S.P., Hagen, S.J., Kanauchi, O., Motoki, K., Sakai, T., Terhorst, C., Koezuka, Y., Podolsky, D.K., Blumberg, R.S., 2000. Activation of natural killer T cells by alpha-galactosylceramide in the presence of CD1d provides protection against colitis in mice. Gastroenterology 119, 119–128.

Seddon, J.M., Cevc, G., Marsh, D., 1983. Calorimetric studies of the gel-fluid (L_β-L_α) and lamellar-inverted hexagonal (L_α-H_{II}) phase transitions in dialkyl- and diacylphosphatidylethanolamines. Biochemistry 22, 1280–1289.

Seddon, J.M. 1990. Structure of the inverted hexagonal (HII) phase, and non-lamellar phase transitions of lipids. Biochimica et Biophysica Acta. 1031 (1): 1–69.

Seddon, J.M., Hogan, J.L., Warrender, N.A., Pebay-Peroula, E., et al., 1990. Structural studies of phospholipid cubic phases. Prog. Coll. Polym. Sci. 81, 189–197.

Seddon, J.M., Zeb, N., Templer, R.H., McElhaney, R.N., Mannock, D.A., 1996. An Fd3m lyotropic cubic phase in a binary glycolipid/water system. Langmuir 12, 5250–5253.

Sen, A., Williams, W.P., Quinn, P.J., 1981. The structure and thermotropic properties of pure 1,2-diacylgalactosylglycerols in aqueous systems. Biochim. Biophys. Acta 663, 380–389.

Sen, A., Mannock, D.A., Collins, D.J., Quinn, P.J., Williams, W.P., 1983. Thermotropic phase properties and structure of 1,2-distearoylgalactosylglycerols in aqueous systems. Proc. Roy. Soc. Lond. B218, 349–364.

Sen, A., Hui, S.W., Mannock, D.A., Lewis, R.N.A.H., McElhaney, R.N., 1990. The physical properties of glycosyl diacylglycerols. 2. X-ray diffraction studies of a homologous series of 1,2-diacyl-3-*O*-(α-D-glucopyranosyl)-*sn*-glycerols. Biochemistry 29, 7799–7804.

Singer, M.A., Finegold, L., Rochon, P., Racey, T.J., 1990. The formation of multilamellar vesicles from saturated phosphatidylcholines and phosphatidylethanolamines: morphology and quasi-elastic light scattering measurements. Chem. Phys. Lip. 54, 131–146.

Stahn, R., Zeisig, R. 2000. Cell adhesion inhibition by glycoliposomes: effects of vesicle diameter and ligand density. Tumour Biol. 21 (3): 176–86.

Tate, M.W., Gruner, S.M., Eikenberry, E.F. 1997. Coupling format variations in X-ray detectors based on charge coupled devices. Rev. Sci. Instr. 68: 47–54.

Tenchova, R., Tenchov, B., Hinz, H.-J., Quinn, P.J., 1996. Lamellar/non-lamellar phase transitions in synthetic glycoglycerolipids studied by time resolved synchrotron radiation. Liq. Cryst. 20, 469–482.

Turner, D.C., Wang, Z.-G., Gruner, S.M., Mannock, D.A., McElhaney, R.N. 1992. Structural study of the inverted cubic phases of di-dodecyl alkyl-β-D-glucopyranosyl-racglycerol. J. Physique 2: 2039–2063.

Tsuji, Y., Fukuda, H., Iuchi, A., Ishizuka, I., Isojima, S., 1992. Sperm immobilizing antibodies react to the 3-*O*-sulfogalactosyl residue of seminolipid on human sperm. J. Reprod. Immunol. 22, 225–236.

van Boeckel, C.A.A., Visser, G.M., van Boom, J.H., 1985. Synthesis of phosphatidyl-β-glucosyl glycerol containing a dioleoyl diglyceride moiety. Application of the tetraisopropyldisiloxane-1,3-diyl (TIPS) protecting group in sugar chemistry. Part IV. Tetrahedron 41, 4557–4565.

Varki, A., Cummings, R., Esko, J., Freeze, H., Hart, G., Marth, J. (Eds.), 1999. Essentials of Glycobiology. Cold Spring Harbor Laboratory Press, New York. ISBN 0-87969-560-9.

Vogel, J., Bendas, G., Bakowsky, U., Hummel, G., Schmidt, R.R., Kettmann, U., Rothe, U. 1998. The role of glycolipids in mediating cell adhesion: a flow chamber study. Biochim Biophys Acta. 1372 (2): 205–15.

Zhao, X., Wakamatsu, Y., Shibahara, M., Nomura, N., Geltinger, C., Nakahara, T., Murata, T., Yokoyama, K.K., 1999. Mannosylerythritol lipid is a potent inducer of apoptosis and differentiation of mouse melanoma cells in culture. Cancer Res. 59, 482–486.